

UNDERGROUND MUON SPECTRUM AT ~40 METER WATER EQUIVALENT

M. I. DAION and L. I. POTAPOV

P. N. Lebedev Physics Institute, Academy of Sciences, U.S.S.R.

Submitted to JETP editor July 30, 1958

J. Exptl. Theoret. Phys. (U.S.S.R.) 36, 697-706 (March, 1959)

A magnetic spectrometer was used to measure the momentum spectrum of muons at a depth of ~ 40 m water equivalent in the $2 \times 10^8 - 5 \times 10^{10}$ ev/c momentum range.

1. INTRODUCTION

MUON momentum spectra at sea level and on high mountains have been the subject of many experimental investigations. The most complete results, based on the largest statistical material, have been recently obtained by Alikhanyan and Alikhanov,^{1,2} Owen and Wilson,³ Caro et al.,⁴ and Kocharyan et al.^{5,6} through magnetic analysis of cosmic radiation by the magnetic mass spectrometer method. At sea level the muons comprise the main part of the penetrating component of cosmic radiations. According to Owen and Wilson, not more than 1% of the total intensity is due to protons. Underground, the nucleon component is rapidly absorbed and at depths greater than 8 or 10 meters of earth the penetrating component of cosmic rays consists of muons.

Usually, when necessary, the muon spectrum at a given depth underground is determined from the known muon spectrum at sea level. Approximating the sea-level spectrum at energies $\gtrsim 10^{10}$ ev by

$$N(p) dp = p^{-\gamma} N_0 dp,$$

where p is the particle momentum and $\gamma \approx 2.7 - 3.0$, we obtain for the spectrum at a depth h

$$N(p) dp = (p + p_0)^{-\gamma} N_0 dp \quad (1)$$

(see, for example, references 7 and 8). Here p_0 is the momentum lost by a muon in passing through a layer of earth of thickness h .

Until comparatively recently there were no direct measurement of momentum spectra underground. We note that measurement of the spectra underground is a rather complicated matter: the construction of mass spectrometers is difficult under such conditions for technical reasons, and the use of other methods does not provide the necessary statistical material (see below).

Recently the problem of the underground muon spectrum has assumed great significance in con-

nnection with the investigation of the interaction between muons and matter, since usually an extrapolation of spectrum (1) is used to calculate various cross sections — production of δ electrons, stars, cascades, or anomalous scattering. The anomalous scattering of muons is of basic significance, and from this point of view the direct measurement of the muon spectrum at relatively low energies is of great interest. Actually, the observed excess scattering could be explained, were the true number of slow muons at a given depth to exceed that calculated by Eq. (1). We note that when determining the intensity of slow muons at a given depth from data obtained from the number of muons at sea level it is necessary, generally speaking, to consider not only the ionization energy losses that this formula accounts for, but several other factors, such as scattering of slow muons in the ground, etc.

The first reports of attempts at direct measurement of the momentum spectrum of muons underground were not published until 1956. George and Shrikantia⁷ give the muon spectrum in the momentum range from 100 to 4,000 Mev/c, obtained experimentally from muon scattering in a photo-emulsion exposed at 57 m water equivalent (w.e.). Compared with the spectrum calculated for this depth from the sea-level spectrum, this spectrum exhibits a considerable particle excess in the energy range from 1 to 5 bev and a deficit in the energy range from 5 to 20 bev. George and Shrikantia believe, however, that this discrepancy cannot be seriously considered, since the accuracy of the data is small.

The spectrum in the low-energy region, $E < 10^9$ ev, was analyzed in connection with the problem of the anomalous scattering. Here, however, by virtue of the small statistical accuracy, no conclusion can be reached concerning the type of the spectrum. George and Shrikantia noted that in spite of the long time covered by the investigation

(more than two years), the material gathered was quite meager, merely 317 trajectories included in the spectrum, and the statistical accuracy of the results could hardly be increased with the photoemulsion method.

Nash and Pointon⁹ determined the muon spectrum at 40 m w.e. in the energy range of $\sim 2 - 8 \times 10^8$ ev, using experimental data on meson scattering in two lead plates placed inside a cloud chamber. Here, unlike the preceding investigation, where the momentum of each particle was determined, the spectrum was plotted on the basis of a statistical treatment of the experimental scattering data, with allowance for the known distribution function of the scattering angles. The calculation was based first on the assumed muon spectrum at a given depth, and the most probable form of the spectrum was then determined by successive approximation.

In the spectrum obtained by Nash and Pointon, the total number of particles with energies 0.5 — 1.0 Bev agrees with the expected value at the given depth of observation, provided the spectrum measured at sea level is suitably transformed. In the momentum range from 2 to 7.5×10^8 ev/c there is also a qualitative agreement in the general form of the spectra. However, the results of this paper pertain to a rather narrow muon energy range and give only a qualitative idea of the form of the spectrum in this region.

In 1956 the underground laboratory of the Moscow State University initiated research on the muon momentum spectrum at a depth of 40 m w.e. by the most direct method, magnetic analysis of cosmic radiation with the aid of an Alikhanyan-Alikhanov mass spectrometer. We describe below the experimental setup and the results.

2. DESCRIPTION OF APPARATUS

We list here only the salient features of the apparatus, since a detailed description of similar setups can be found in the literature (references 1, 5, 10, etc.).

A diagram of the instrument is shown in Fig. 1. In the electromagnet gap (measuring $20 \times 60 \times 10$ cm) are located six trays of counters 1, 2, 3, I, II, and III. Three trays of small-diameter counters, i. 2, 3, permit measurement of the radius of the curvature and thus the momentum of the particle. The tray marked O_m is for monitoring purposes. Four other monitoring trays O_{lin} , I, II, and III serve to check the linearity of the trajectory in the plane B. Located under the gap are absorbers IV, V, VI, and VII, and counter trays that determine the ranges of the particles. In the case of

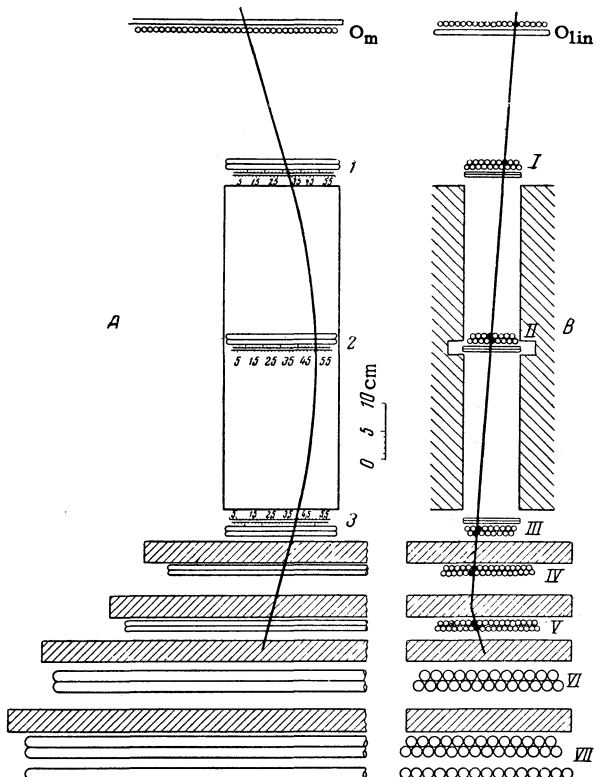


FIG. 1. Diagram of the instrument.

hard particles that pass through all the absorbers, they provide additional control over the linearity of the trajectory in the plane B.

The arrangement of the counters in trays 1 — 3, I — III is shown in the same Fig. 1. Table I lists the counter data. The electronic portion of the apparatus consisted of a coincidence block and a hodoscopic system GK-7,¹¹ controlled by a 1 + 2 + 3 coincidence pulse. Before the start of the investigation, the entire counter system was thoroughly adjusted and the adjustment was checked by a special series of measurements performed without a magnetic field. These control measurements were repeated frequently.

During the actual measurements, the direction of the magnetic field in the gap was reversed twice a day, whenever the films were changed.

TABLE I

Number of trays	Counter diameter, mm	Counter length, mm	Cathode material	Number of counters in tray	Wall thickness, mm
O_m	10	200	Cu	50	0.15
I	4.8	100	Al	59	0.1
2	4.8	100	Al	59	0.1
3	4.8	100	Cu	59	0.1
O_{lin}	10	550	Cu	18	0.15
I	8	200	Al	19	0.15
II	8	200	Al	17	0.15
III	10	200	Cu	15	0.15
IV	10	450	Cu	33	0.15
V	10	550	Cu	37	0.15
VI	20	800	Cu	25	0.15
VII	20	900	Cu	42	0.15

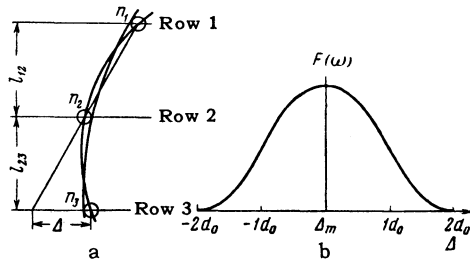


FIG. 2.a) Determination of the deviation Δ of the particle from the initial direction; b) Shape of the distribution function of the values of Δ .

3. PROCESSING OF THE DATA

We shall deal in somewhat greater detail with the processing of the experimental data, since our method differs from that used in most similar investigations.

It is known that the system makes it possible to identify the counters through which a particle has passed by the flashing of corresponding neon lamps. However, the placement of the counters does not determine uniquely the radius of the circular trajectory of the particle since a given combination of counters may lie in the path of trajectories of various curvatures.

We introduce a quantity Δ , uniquely related with the radius of curvature ρ of the particle trajectory (see Fig. 2a). In a narrow long telescope, the following relation between ρ and Δ is satisfied, with good approximation:

$$\rho = (L^2 + \Delta^2)/4\Delta, \quad (2)$$

where $L = l_{12} + l_{23}$. The distribution function of the quantity Δ within the counter combination characterized by the quantity $\Delta_m = md$ can be represented in the following form¹²

$$F(\omega) = \begin{cases} 2(1/\omega - \omega^2), & 0 \leq |\omega| \leq 1/2, \\ 2(1 - |\omega|)^2, & 1/2 \leq |\omega| \leq 1, \end{cases} \quad (3)$$

where $\omega = (\Delta - \Delta_0)/2d$.

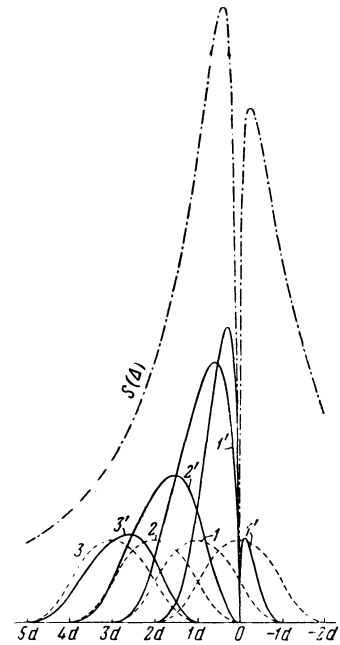
In our case $d = d_0/3$, where d_0 is the counter diameter. A plot of this function is shown in Fig. 2b. This yields a statistical error of $0.26 \times 2d$ in the determination of Δ , and a relative error

$$(\delta\Delta/\Delta)_{\text{prob}} = 0.26 \cdot 2d/\Delta.$$

For large values of Δ , the error is small and therefore in determining the spectrum in this region (for small ρ) the radius of curvature of each trajectory is determined from the positions of the centers of the corresponding counters,* and the momentum of the particle is calculated from the formula $p = 300 H\rho$.

*We shall not dwell on the method of calculating the radius.

FIG. 3. Arrangement of the primary beam by deviation categories.



The data obtained for small values of $\Delta_m = md$ were processed with allowance for the distribution function (3).* The method used can be most clearly explained with the aid of Fig. 3. Here the abscissas represent the deviations of Δ . The quantities $1d, 2d, 3d, \dots$ correspond to experimentally-obtained categories of deviations $\Delta_m = md$ ($m = 1, 2, 3, \dots$). The dotted curves show the distribution functions of Δ within each category Δ_m (and are so marked). The same diagram shows the spectrum of the particles incident on the apparatus (dash-dot line).

To determine the probability of entrance of particles with a deviation Δ in category Δ_m , the ordinate of the spectrum for given must be multiplied by the corresponding ordinate of the distribution function (more accurately, taking normalization into account, by a quantity equal to half the ordinate). The curves $1', 2', 3' \dots$ thus obtained give the actual distribution relative to the deviations inside each category of deviations [for a specified primary spectrum $s(\Delta)$].

This raises the question of how the total number of particles N_m , registered in a given category of deviations m (N_m is proportional to the area under curve m') can be used to determine the primary spectrum in this energy range. In investigations where the distribution function is not taken into account, it is essentially assumed that any deviation category corresponds to a deviation interval

$$\Delta_m - d/2 \leq \Delta \leq \Delta_m + d/2. \quad (4)$$

*An analysis of spectra with use of the distribution function is contained in reference 3.

TABLE II

Δ_m	$p_m^{(1)}$, Bev/c	H = 6300 oe			H = 3300 oe			
		σ			σ			
		$\gamma = 2.5$	$\gamma = 2.8$	$\gamma = 3.0$	$\gamma = 2.5$	$\gamma = 2.8$	$\gamma = 3.0$	
1	2	3	4	5	6	7	8	
1/4 d	49.5	1.67	1.92	2.1	26	1.42	1.47	1.7
1 d	12.5	0.7	0.66	0.63	6.5	0.86	0.77	0.72
2 d	6.18	~1	~1	~1	3.25	1.14	1.10	1.08
3 d	4.42	~1	~1	~1	2.17	1.08	1.07	1.06
4 d	3.08	~1	~1	~1	1.62	1.06	1.05	1.05
5 d	2.47	~1	~1	~1	1.31	~1.03	~1.03	~1.03

The average number of particles \bar{n}_m per unit momentum interval is determined, for example, by dividing the total number of particles N_m by the momentum interval corresponding to the deviation interval (4). The resultant value is usually associated, without additional justification, with the momentum p_m corresponding to the center of the category Δ_m (or to the center of the momentum interval). Calculation based on the foregoing scheme of subdividing the primary spectrum into deviation categories shows that the resultant values \bar{n}_m must be subjected to corrections that are different for different deviation categories and depend, furthermore, on the type of the original spectrum.

The corrections were calculated for several initial spectra (see below). In each case curves similar to those shown in Fig. 3 are used to determine the values of \bar{n}_m by calculating the areas under the curves m' and dividing these areas by the momentum interval corresponding to the deviation interval (4). (This corresponds to the method used to obtain the value of n_m from the experimental data). The resultant values of \bar{n}_m were compared with the true value of the average number of particles per unit momentum interval n_{sp} in the initial spectrum, $S(\Delta)$, at the point Δ_m . The $\sigma_m = \bar{n}_m/n_{sp}$ shows by how much the values of \bar{n}_m obtained with this method of data processing exceed the true values.

4. EXPERIMENTAL RESULTS

Before starting the investigation, a special experiment was set up to measure the intensity of the hard component ($p \gtrsim 3.5 \times 10^8$ ev/c) at sea level (I_0) and at our depth (I_h), using a telescope that subtends the same angle as the telescope of the mass spectrometer. Based on the obtained $I_0/I_h = 11.13 \pm 0.43$ and on the known spectrum of the muons at sea level,⁴ the value of p_0 was determined from the condition that the number of particles in the spectrum⁴ with momenta greater than p_0 constitutes $1/11.13$ of the total number of particles in the spectrum. Such an estimate

yields $p_0 \approx 9.8$ Bev/c, which may be somewhat of an underestimate. Other methods of determining these quantities lead approximately to the same value of p_0 . Since the absolute intensity of the hard component at sea level is $0.83 \times 10^{-2} \text{ cm}^{-2} \text{ sec}^{-1} \text{ sterad}^{-1}$, the intensity at our depth was assumed to be $0.83/11.13 = 0.745 \text{ cm}^{-2} \text{ sec}^{-1} \text{ sterad}^{-1}$; the spectrum obtained by us was normalized to this value of absolute intensity (see below).

It is natural to expect that in the momentum range of interest to us the underground muon spectrum would be described, at least approximately, by Eq. (1) with $\gamma \sim 2.5$ to 3.0. Our calculations for σ_m were therefore based on the spectrum (1). Since, for a given p , the deviation Δ depends on the value of the magnetic field H ($p \sim 300 \text{ HL}^2/4\Delta$), the corrections σ_m were calculated for two versions of the experiment: one with a 6300 oe magnetic field (first series of measurements) and one measured at 3300 oe (second series of measurements), and in each case for $\gamma = 2.5$, 2.8, and 3.0.

The values obtained for σ are listed in Table II, from which it is seen that in the first series of measurements the correction plays a noticeable role only for two deviation categories, $\Delta_0 = 0$ and $\Delta_1 = 1$ d, and that the value of σ depends here on the value assumed for γ .* For the categories $\Delta_m \geq 2$ d, the coefficient σ is practically independent of γ . Thus, the method for processing the experimental data in this series of measurements, in the region $\Delta_m \geq 2$ d, is practically independent of the assumed initial muon spectrum. The solid circles in Fig. 4 represent the spectrum we obtained in this range of momenta. The abscissas represent the particle momenta, and the ordinates the absolute intensities within a 1-Mev momentum interval, with allowance for the geometry of the instrument (cf. below).

*In calculating the values of σ_m for the category Δ_0 and Δ_1 we considered that particles of both signs may be included in this category. It was assumed that the spectra of positive and negative mesons are similar and that the positive excess is $n_+/n_- = 1.20$. In the category $\Delta_0 = 0$, the value of σ was calculated at the point $d/4$.

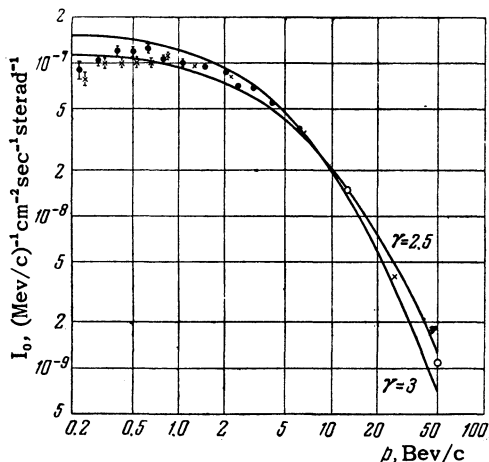


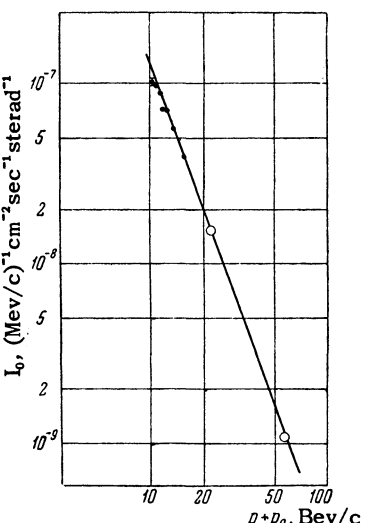
FIG. 4. Comparison of calculated spectra for $\gamma = 2.5$ and $\gamma = 3.0$ with the spectrum obtained for the muons.

Figure 5 shows the same spectrum, for the momentum range $p > 10^9$ ev/c, but at a different scale: the abscissas represent $p + p_0$. It is seen from this that in the momentum range 2×10^9 ev/c $\gtrsim p \gtrsim 10^{10}$ ev/c the spectrum can be approximated by a straight line, whose slope yields $\gamma \approx 2.7 - 2.8$.

If it is assumed that at large momenta, corresponding to the deviation categories $\Delta_m = 0$ or $1d$, the spectrum exponent remains constant, then the corrections listed in column 4 of Table II, and corresponding to $\gamma = 2.8$, should be introduced in the experimental values of \bar{n}_0 and \bar{n}_1 . The intensities obtained with allowance for these corrections are plotted in Figs. 4 and 5 with light dots. It is seen that these two fit well the same straight line. The most probable value of γ , calculated over all points of the spectrum in the region $p \gtrsim 2 \times 10^9$ ev/c, is $\gamma = 2.78 \pm 0.23$. It must be recalled, however, that when $\Delta_m < 2d$ the magnitude of the correction depends on the initial assumptions concerning the shape of the spectrum. Since it is very probable that in this region the true value of the spectrum exponent is greater than the assumed initial value $\gamma = 2.8$, the two last points of the spectrum are only tentative.

In our preceding analysis, the values of \bar{n}_m pertain to the center of the interval Δ_m (only the quantity \bar{n}_0 pertained to the deviation $\Delta =$

FIG. 5. Spectrum of muons in the momentum range $p > 2 \times 10^9$ ev/c.



$d/4$). However, as can be seen from Fig. 3, the maximum number of particles (the maxima of the curves $1'$, $2'$, $3'$, ...) registered within a given category have smaller deviations, Δ_{\max} . The quantities \bar{n}_m can be related to the deviations Δ_{\max} . It is necessary to use, in this case, when plotting the spectrum, other correction coefficients σ'_m , calculated in the same manner as the coefficients σ_m . The spectrum plotted by this method was not found to differ from the one given here.*

Starting with the results of the first series of measurements, the calculations performed in the examination of the data of the second series were based on a spectrum with $\gamma = 2.8$; the values of the corresponding corrections σ are given in column 8 of Table II. For comparison we give also the values of σ at $\gamma = 2.5$ and 3.0 . The spectrum obtained is marked on Fig. 4 by crosses. It is seen that within the limit of statistical errors, the spectra obtained in both series of measurements are the same.

We indicate in the conclusion that the total number of trajectories, selected for the construction of the spectra, is 26,226; of these the spectrum of the first series included 12,740 trajectories, and the spectrum of the new series included 13,486.

Remarks on Allowance for the Aperture Ratio of the Instrument

When we plotted the spectra for small momenta we took into account the aperture ratio of the instrument, which depends both on the geometry of

*Essentially it is more logical to associate the given deviation category Δ not with the momentum p_m , corresponding to the center of the category Δ_m , or with p_{\max} , corresponding to the maximum in the curve showing the Δ distribution, but, say, a momentum p such that the number of particles in the given category, having a momentum less than p , equal the number of particles with momentum greater than p .

TABLE III

p , Bev/c	$H = 3300$ oe			$H = 6300$ oe		
	Aperture ratio			Aperture ratio		
	$n = 1$	$n = 2$	$n = 3$	$n = 1$	$n = 2$	$n = 3$
	1	2	3	4	5	6
0.2	0.95	0.92	0.9	0.78	0.74	0.7
0.4	0.98	0.97	0.96	0.94	0.93	0.91
0.6	0.99	0.98	0.98	0.98	0.97	0.96
0.8	0.99	0.98	0.98	0.99	0.98	0.97
1.0	~1	0.99	0.99	0.99	0.98	0.97
2.0	~1	~1	~1	~1	0.99	0.98
5.0	~1	~1	~1	~1	~1	~1

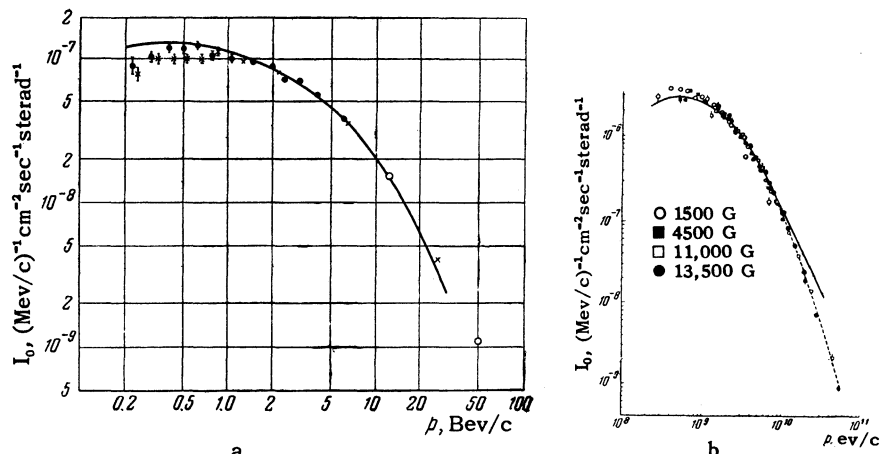


FIG. 6. Comparison of the spectrum obtained with (a) that of Caro et al.,⁴ (b) converted to a depth equivalent to ~ 40 m of water.

the telescope and on the angular distribution of the particles in the beam. There are numerous calculations in the literature for the aperture ratios of the mass spectrometers. Our calculation was based on the method described in reference 10. The angular distribution at our depth of observation in the momentum range from 2 to 7×10^8 ev/c, where it influences the magnitude of the aperture ratio, is represented by the law $I_\theta = I_0 \cos^n \theta$, with $n \sim 2.9$.¹⁴ However, allowance for the scattering of mesons in a lead block placed over the apparatus shows that the value of n will be less for the particle beam registered by this instrument. In view of the weak dependence of the aperture ratio on n , an exact calculation of n was not carried out. In Table III we list the values of the aperture ratio, calculated under the assumption that $n = 2$. We show also for comparison the aperture ratios for $n = 1$ and $n = 3$. In plotting the spectra we used the values of the aperture ratio given in columns 3 and 6 of Fig. 3.

5. DISCUSSION OF THE RESULTS

It is interesting to compare the spectrum obtained with the muon spectrum at sea level and with the customary spectrum approximation as represented by Eq. (1) (see Fig. 6). Figure 6b shows the muon spectrum at sea level, obtained by Caro et al.⁴ Since the muons lose an energy of 9.8 Bev on the path from the surface of the earth to the specified depth, the spectrum of interest to us will be in the region $E > 9.8$ Bev, where the approximation of reference 4 is shown dotted.

We have recalculated the Caro spectrum to our depth, taking into account the indicated muon energy losses in the earth. We also allowed for the change in the widths of the momentum intervals, to which the same particles belong at sea level (dp) and at the given depth (dp_1). The dp_1/dp ratio was calculated from the expression for dR/dp (R is

the particle range) given by Rossi and Greisen.¹⁵ The intensity of the muons having a momentum p at a given depth was determined by dividing the ordinate of the Caro spectrum at the point $p + 9.8$ Bev/c by the quantity dp_1/dp . The results are shown by the solid line in Fig. 6a. If we take into account the statistical errors in the Caro spectrum, we can state that our data agree with the transformed Caro spectrum.

The Owen and Wilson spectrum³ in the region $p \gtrsim 10^{10}$ ev/c lies somewhat above the Caro spectrum (a comparison of the spectra is cited in reference 3), but the Owen and Wilson data are less trustworthy in this momentum region, since they correspond to the zero category of deviations (see section IV).

The spectrum shown in Fig. 4 was obtained from spectra calculated by formula (1), for $\gamma = 2.5$ and 3.0. In both cases the spectra are normalized to the total number of particles in the experimental spectrum.

6. CONCLUSIONS

1. In the momentum range $p \geq 2 \times 10^9$ ev/c, the muon spectrum can be expressed approximated by the formula

$$N(p) dp = N_0 dp / (p + p_0)^\gamma,$$

where $\gamma = 2.78 \pm 0.23$ and $p_0 = 9.8$ Bev/c. The same formula can be used to approximate the spectrum in a wider region, for $p \lesssim 2 \times 10^8$ ev/c.

2. The spectrum obtained leads to the conclusion that the so-called anomalous scattering of muon mesons, observed in many underground investigations, can absolutely not be due to underestimating the number of slow muons.

The authors express their great indebtedness to A. I. Alikhanyan for much help in completing this work, for valuable advice, and for discussion of the results, and also to V. Kh. Volinskikh and

V. Krugovykh for help with the experimental portion of the work. The authors take this opportunity to express gratitude to S. N. Vernov, N. L. Grigorov, and G. B. Khristyansen for affording the opportunity of working at the underground laboratory of the Moscow State University.

¹ Alikhanyan, Alikhanov, and Vaisenberg, J. Exptl. Theoret. Phys. (U.S.S.R.) **18**, 301 (1948).

² A. I. Alikhanyan and A. O. Vaisenberg, J. Exptl. Theoret. Phys. (U.S.S.R.) **32**, 413 (1957), Soviet Phys. JETP **5**, 349 (1957).

³ B. G. Owen and J. G. Wilson, Proc. Phys. Soc. **A68**, 409 (1955).

⁴ Caro, Parry, and Rathgeber, Austral. J. Scient. Res. **A4**, 16 (1951).

⁵ N. M. Kocharyan, Dissertation, Erevan, 1954, Phys. Inst. Acad. Sci. Arm. S.S.R.

⁶ Kocharyan, Aivazyan, Kirokasyan, and Aleksanyan, J. Exptl. Theoret. Phys. (U.S.S.R.) **30**, 243 (1956), Soviet Phys. JETP **3**, 350 (1956).

⁷ E. P. George and G. S. Shrikantia, Nucl. Phys. **1**, 54 (1956).

⁸ D. Kessler and R. Maze, Nuovo cimento **5**, 1940 (1957).

⁹ F. W. Nash and A. J. Pointon, Proc. Phys. Soc. **A69**, 725 (1956).

¹⁰ Daion, Fedorov, Merzon, and Shostakovich, Приборы и техника эксперимента (Instruments and Measurement Engineering) No. 1, 3 (1957).

¹¹ Новые применения ламп с холодным катодом в импульсной аппаратуре (New Application of Cold Cathode Tubes in Pulse Apparatus), VINITU press, 1956.

¹² Hyams, Mylroi, Owen, and Wilson, Proc. Phys. Soc. **A63**, 1053 (1950).

¹³ B. Rossi, Revs. Modern Phys. **20**, No. 3, 1948.

¹⁴ Cousins, Nash, and Pinton, Nuovo cimento **6**, 1113 (1957).

¹⁵ B. Rossi and K. Greisen, Revs. Modern Phys. **13**, 240 (1941).

Translated by J. G. Adashko
131